Published in final edited form as:
Mol Cancer Res. 2007 August ; 5(8): 813–822. doi:10.1158/1541-7786.MCR-07-0104.

ATM-dependent DNA damage checkpoint functions regulate gene expression in human fibroblasts

Tong Zhou[1], **Jeff Chou**[2], **Yingchun Zhou**[1], **Dennis A. Simpson**[1], **Feng Cao**[1], **Pierre R. Bushel**[2], **Richard S. Paules**[2], and **William K. Kaufmann**[1,*]

[1]Department of Pathology and Laboratory Medicine, Center for Environmental Health and Susceptibility, and Lineberger Comprehensive Cancer Center, University of North Carolina at Chapel Hill

[2]National Institute of Environmental Health Sciences, Research Triangle Park, NC

Abstract

The relationships between profiles of global gene expression and DNA damage checkpoint functions were studied in cells from patients with ataxia telangiectasia (AT). Three telomerase-expressing AT fibroblast lines displayed the expected hypersensitivity to ionizing radiation (IR) and defects in DNA damage checkpoints. Profiles of global gene expression in AT cells were determined at 2, 6 and 24 h after treatment with 1.5 Gy IR or sham-treatment, and were compared to those previously recognized in normal human fibroblasts. Under basal conditions 160 genes or ESTs were differentially expressed in AT and normal fibroblasts, and these were associated by gene ontology with insulin-like growth factor binding and regulation of cell growth. Upon DNA damage, 1091 gene mRNAs were changed in at least two of the three AT cell lines. When compared with the 1811 genes changed in normal human fibroblasts after the same treatment, 715 were found in both AT and normal fibroblasts, including most genes categorized by gene ontology into cell cycle, cell growth and DNA damage response pathways. However, the IR-induced changes in these 715 genes in AT cells usually were delayed or attenuated in comparison to normal cells. The reduced change in DNA-damage-response genes and the attenuated repression of cell-cycle-regulated genes may account for the defects in cell cycle checkpoint function in AT cells.

Keywords

ATM; cell cycle checkpoint; ionizing radiation; microarray

Introduction

Inactivating mutations in the *ataxia telangiectasia-mutated* (*ATM*) gene lead to radiation hypersensitivity, defects in DNA damage checkpoint functions, and chromosomal instability (1–3). DNA damage, such as ionizing radiation (IR)-induced double-strand breaks (DSB), triggers auto- or trans-phosphorylation of serine 1981 of ATM leading to the dissociation of inactive ATM dimers into catalytically active ATM monomers (4). The rapid activation of ATM after even very low doses of IR appears to be a response to an alteration of chromatin structure (4). More than 400 mutations in this large gene (62 exons spanning ~150 kb) have been documented in AT patients, of which about 70% are truncating mutations and 30% are

[*]**Corresponding author**: Department of Pathology and Laboratory Medicine, Lineberger Comprehensive Cancer Center, CB#7295, University of North Carolina at Chapel Hill, Chapel Hill, NC 27599-7295, USA, Tel: 919-966-8209, Fax: 919-966-9673, wkarlk@med.unc.edu.

missense mutations (5–8). Although all the mutations affect ATM functions in DNA damage response and cell cycle checkpoint control, mutations of different subtypes may show different responses to DNA damage. *ATM* heterozygous cell lines with truncation mutations had higher cell survival after exposure to 2 Gy irradiation compared to those with missense mutations (6).

ATM-dependent, post-translational modification of protein structure and function has been widely studied in DNA damage responses (1, 2, 9, 10). In addition to defects in DNA damage response, the absence of normal ATM in AT cells may affect cell proliferation by interfering with cytoplasmic signaling pathways and accelerating telomere shortening (3, 11, 12). Changes in transcription factors have been reported in AT cells, including activated NF-κB, AP-1, p53 and Rb/E2F pathways (13), and defective CREB transcriptional activity (14). Fibroblasts from AT patients usually grow more slowly than normal fibroblasts. This may be due to lower levels of IGF-1R (13). The progeroid-like phenotype of AT patients may be related to disregulation of the somatotroph axis that includes IGF and IGF-1R (15, 16). AT fibroblasts may undergo earlier senescence compared with normal fibroblasts (17–19). Accelerated telomere erosion seen in AT cells may be associated with the normal function of ATM to signal deprotected telomeres during G2 (18–20). ATM thus appears to have important roles in regulation of many transcriptional signaling pathways that are related to cell growth and DNA damage responses.

Recent effort has examined ATM-dependent transcriptional regulation using microarray technology (3, 13, 21–23). A comprehensive determination of global gene expression in AT cells will contribute to understanding the functions of ATM in cell proliferation and cell cycle regulation. Global gene expression may also assist in the identification of *ATM* heterozygotes with increased risk of breast and other cancers (24). In the present study, we quantified DNA damage checkpoint functions and global gene expression profiles in fibroblast lines from three different AT patients. To reduce concern about accelerated telomere erosion and premature senescence in AT skin fibroblasts, the catalytic subunit of telomerase, hTERT, was transduced to induce expression of telomerase and stabilize telomeres. In comparison to telomerase-expressing normal fibroblasts, hypersensitivity and attenuated DNA damage checkpoint function in IR-treated AT fibroblast lines was clearly associated with attenuated changes in global gene expression.

Results

Radiation hypersensitivity and defective DNA damage checkpoint functions in AT lines

Based on information from the Coriell Institute, AT1 has a transition mutation (103C-T) in *ATM* that results in a stop codon at position of 35 of the ATM protein; AT2 has two truncating mutations, one at nucleotide 1548 on the paternal allele, the other at nucleotide 1978 on the maternal allele. The mutation in AT3 is not known. Western immunoblot analysis of ATM protein expression showed that ATM was expressed in three normal fibroblast lines while very little or no ATM protein was observed in the three AT fibroblast lines (Figure 1A).

The three AT fibroblast lines displayed single-cell colony formation efficiencies of 10–15%. When plated at single-cell densities the AT lines were hypersensitive to IR-induced inhibition of colony formation. Colony inactivation curves for telomerase-expressing AT and normal fibroblasts were comparable to those previously reported for fibroblasts that were not transduced with hTERT (25, 26). The 1.5 Gy IR dose reduced clonal expansion by 85–92% in the AT lines (AT1, AT2 and AT3). Clonal expansion was reduced by only 40–45% by the same dose of IR in normal human fibroblasts (F1, F3 and F10) (Figure 1B, data for normal fibroblasts taken from (27)).

The G1 checkpoint response to IR was quantified by measuring the incorporation of BrdU 6–8 h after 1.5 Gy or sham-treatment. G1 checkpoint function was severely attenuated in AT cells (Figure 1C) with only small IR-induced reductions (5–13%) in the fraction of BrdU-labeled S phase cells, confirming that the immediate G1 checkpoint response to IR is ATM-dependent (10, 28, 29). The IR-induced G2 checkpoint was quantified by measuring mitosis-specific phospho-histone H3 immunostaining 2 h after IR- or sham-treatment (Figure 1C). IR-treated AT fibroblasts displayed a G2 arrest as indicated by the 32–42% reduction in the fraction of mitotic cells. However, in comparison to the >90% reduction in mitotic cells in IR-treated normal fibroblasts (27), the AT fibroblasts also displayed significant attenuation of G2 checkpoint function. Thus, although ATM is required for the G2 checkpoint response to IR-induced DNA damage, AT cells are nevertheless partially able to delay the G2/M transition after IR treatment.

The time-course of changes in cellular DNA content, DNA synthesis and mitosis in normal and AT cells indicated that the fraction of BrdU-labeled S phase cells was little affected by IR at 2 h post-treatment in both normal and AT cells, it was reduced by 50% in normal cells and by 5–8% in AT cells at 6 h after IR, and it was reduced by about 90% and 60% in normal and AT lines, respectively, by 24 h after IR (Figure 2A). The reduction in S phase cells was associated with an increase in G2 cells and persistent fractions of G1 cells. Thus, AT cells displayed evidence for delays in G1 and G2 by 24 h after IR. The mitotic indices of normal cells were severely reduced by over 95% at 2 h after IR irradiation, recovered to control levels at 6 h, and then fell again to 30% of control at 24 h. Unlike the normal fibroblasts, the mitotic indices of AT cells were reduced by 32–42% 2 h after IR and remained at this level relative to sham-treated controls for up to 24 h in the AT1 and AT3 lines. In AT2 cells the mitotic index also remained at reduced levels 2–6 h after IR but recovered to 170% of the control level at 24 h (Figure 2B).

ATM-dependent gene expression profiles with or without DNA damage

In a previous experiment, changes in gene expression in response to IR-induced DNA damage were determined in three telomerase-expressing, normal human fibroblast lines using Agilent Human 1A arrays (27). The same microarray platform and experimental analyses were used to monitor gene expression in AT cell lines. Because gene expression in normal and AT cells was determined relative to a universal reference RNA, it was possible to identify genes with different levels of expression in the two classes of cells (normal vs AT). Using the EPIG method for identification of differentially expressed genes (Chou J, Zhou T, Kaufmann WK, Paules RS, Bushel PR. “Extracting gene expression patterns and identifying co-expressed genes from microarray data”, submitted for publication), 229 genes or ESTs were found to be expressed differently in AT and normal fibroblasts growing under basal conditions. However, one important factor that needed to be considered in this comparison was that normal fibroblasts were cultured in DMEM with 10% FBS while AT fibroblasts were cultured in DMEM with 20% FBS or AmnioMAX™-C100 medium (see Materials and Methods). Differences in culture condition may have contributed to the differential gene expression. Consequently, a second experiment was done with two normal human fibroblast lines, F1 and F10, and two AT fibroblast lines, AT1 and AT2, cultured in the same medium (DMEM with 20% FBS) and microarray analysis were performed again for determination of differential gene expression. Of the 229 genes first found to differ between normal and AT lines, 160 were further confirmed to be differentially expressed in the second experiment, of which 88 genes were down-regulated and 72 genes were up-regulated in AT cells compared to normal cells (see Supplement 1 for gene list). Gene ontology (GO) analysis of these genes identified three significantly over-represented categories: insulin-like growth factor binding, histogenesis and organogenesis, and regulation of cell growth. The insulin-like growth factor binding category included *IGFBP3,*

IGFBP5, NOV, PRSS11 and *WISP2*. This result is consistent with previous studies demonstrating abnormal regulation of IGF1 and IGF1-R in AT fibroblasts (22).

Gene expression at 2, 6 and 24 h after IR-treatment and 6 h after sham-treatment was determined in AT cell lines. Four patterns of IR-induced changes in gene expression were identified by EPIG, affecting 349 genes in all three AT lines (Figure 3, see Supplement 2 for gene lists). Among the four expression patterns in AT cells, early-induced and early-repressed patterns 1 and 2 included only 9 and 6 genes, respectively, while late-induced and late-repressed patterns 3 and 4 with 109 and 225 genes, respectively, accounted for most of the gene expression changes induced by IR. The late-induced gene list included the targets of p53 transactivation, *CCNG1, PA26* and *TP53TG1.* Many G1/S transition-regulated genes such as *CDC45L, CDC6, CDC7L1, CDK2, E2F1, MCM2, MCM3, MCM5, MCM6, MCM7, PCNA, POLA2, POLD1, POLE3, RFC2, RFC4* and *RFC5* were included in the late-repressed gene list. When compared with normal human fibroblasts that had 1811 IR-responsive genes falling into 9 patterns of response (27), many DNA damage-responsive genes in normal fibroblasts, including p53 target genes *CDKN1A, GADD45A, SES2, BTG2, SNK, PPM1D, CNK, PLAB, BAX, DDB2* and *TP53INP1* (27), were not found to have significant changes in AT lines after IR-treatment, nor were many late-repressed G2/M transition-regulated genes identified in AT cells, such as *CCNB1, CCNB2, CDC20, CDC25C* and *TOP2A*.

Further analysis of the expression of these genes in irradiated AT cell lines revealed that p53 target genes were induced by IR in AT2 and AT3 in a delayed pattern as has been previously reported (22, 30), but these genes displayed little change in AT1 (Figure 4A). Analysis of these genes in three normal fibroblast lines indicated that some genes, such as *CDKN1A*, *FDXR*, *1000314* and *SNK,* were highly induced at the 2 h time point and others, such as *BAX*, *CES2*, *DDB2* and *OSBPL3*, displayed later induction at 6 and 24 h as in AT2 and AT3 (Figure 4B). The G2/M transition-regulated genes that were strongly repressed in normal cells (Figure 4D) were moderately repressed in AT1 and AT3 at 24 h post-IR but not in AT2 (Figure 4C). This observation was consistent with the observed persistent repression of mitotic index in AT1 and AT3 but not AT2 cells at 24 h post-IR treatment (Figure 2). These results indicate that changes in gene expression profiles upon DNA damage are closely associated with the unique alterations in cell cycle progression and checkpoint responses that are seen in individual AT fibroblast lines.

Although all ATM mutations significantly attenuated G1 and G2 checkpoint functions in our three AT cell lines, each line displayed unique features of cell cycle progression after DNA damage. These inter-individual differences may account for the differences in clinical features of the disease among AT patients (31). In order to observe as many ATM-related effects on global gene expression upon DNA damage as possible, additional EPIG analyses were done to identify IR-induced changes in gene expression that occurred in two out of three AT cell lines. Each of the combinations of AT1/AT2, AT2/AT3, and AT1/AT3 produced the same four expression patterns (Figure 3) seen with all three lines. However, the sum of significant genes from all combinations increased to 1091 (see Supplement 3 for gene list), a number still less than the 1811 IR-responsive genes seen in normal fibroblasts. Comparison of the two sets of genes showed that 715 genes (see Supplement 4 for gene list) responded to IR-induced DNA damage in both AT and normal fibroblasts. Gene ontology (GO) analysis of these 715 IR-responsive genes covered more than 80 categories of biological processes, cellular components or molecular function of which most were related to cell cycle regulation and DNA damage response with the top 10 categories of biological process being concerned with DNA replication, mitosis and cell division. GO analysis of the 1096 genes (see Supplement 5 for gene list) that responded specifically in normal fibroblasts identified 13 categories including DNA repair, response to DNA damage stimulus, and cell

cycle checkpoint. For the 376 genes (see Supplement 6 for gene list) that responded to IR specifically in AT fibroblasts, two biological processes, cell communication and morphogenesis were over-represented in GO analysis. Furthermore, combined EPIG analysis of gene expression profiles from all AT and normal cell lines was performed. The six expression patterns that were identified indicated that IR-induced changes in gene expression were delayed or attenuated in AT cells compared to normal cells (Figure 5, see Supplement 7 for gene list).

Discussion

ATM has been shown to have important roles in the transcriptional regulation of gene expression by phosphorylation of transcription factors such as p53, NF-κB, E2F, CREB and BRCA1, and in maintenance of the normal functions of IGF-1R and telomeres (3, 13, 14, 32). ATM-dependent gene expression has been systematically studied by comparing cell lines from normal individuals and AT patients, isogenic cell lines with restoration of ATM in AT cells or siRNA knock-down of ATM in wildtype cells, and $ATM^{+/+}/ATM^{-/-}$ mice (3, 13, 21–23). More than 300 genes have been reported to display ATM-dependent expression although few genes were commonly identified in two or more experiments. The microarray results presented here identified 160 genes or ESTs (about 1% of the total on the array) that were differentially expressed in normal and AT fibroblast lines under basal growth conditions, of which about half were up-regulated and half were down-regulated in AT cells relative to normal cells. Three gene ontology categories, insulin-like growth factor binding, histogenesis and organogenesis, and regulation of cell growth, were over-represented in these genes. The normal and AT lines did differ in growth rates as the average S fractions were 35% in the normal lines growing in medium with 10% FBS and 25% in the AT lines growing in medium with 20% FBS or Amniomax medium with 10% FBS. Similarly, the average mitotic indices were 2% in normal lines and 1.5% in AT lines. It is notable that a previous study demonstrated that ATM regulates expression of insulin-like growth factor-1 receptor (IGF-1R) and signaling through the IGF-1R contributes to radioresistance (32). ATM is also known to phosphorylate the same ser111 residue on 4E-BP1 that is induced by insulin (33). Reduced expression of the important IGF-1 receptor in AT lines may account for their reduced growth rate in comparison to the normal lines. The results presented here indicated that ATM also regulates the expression of several genes that are associated with insulin-like growth factor binding. Enhanced expression of *IGFBP3* in AT cells can inhibit cell growth directly or by competitively binding IGF's and preventing their binding to the IGF-IR (34). Endocrine dysfunction involving insulin-like growth factors is associated with neurodegeneration in humans and animal models (35). The observation that AT cells differ from the normal cells in the expression of several genes that participate in insulin-like growth factor signaling supports a hypothesis that abnormalities in insulin-like growth factor signaling may contribute to neurodegeneration in AT.

The ATM-dependent, DNA-damage-responsive patterns of gene expression have also been studied in many experiments (13, 21–23, 30, 36, 37). Unlike the large variation among experiments for determination of ATM-dependent expression in the absence of DNA damage, the same sets of ATM-dependent DNA damage responsive genes were reproducibly observed in the current and previous studies. At early times between 2 to 10 h after treatment with relatively low doses of IR, genes that function in cell cycle checkpoints and DNA repair are usually not induced, or are less-well-induced in AT cells compared to normal cells. Many of these genes are p53-target genes, such as *CDKN1A, DDB2, GADD45a CCNG* and *BAX*. Some E2F-regulated genes, such as *RFC* subunits, *MCM* family members, *CCNA, CCNB* and *PCNA* were repressed to a lesser extent in AT cells (22–24). It should be noted that the dose of IR-induced DNA damage can markedly affect the identification of ATM-dependent gene expression. For example, while AT and normal

lymphoblasts showed clear differences in expression of the above-mentioned genes after 1 Gy IR, after 5 Gy IR the differences of gene expression were eliminated, apparently because ATR signaling was activated in AT lymphoblasts after the higher dose and initiated similar checkpoint functions as in normal cells (30). In the present analysis, a 1.5 Gy IR dose that inhibited clonal expansion by 90% in AT fibroblasts and 40% in normal human fibroblasts (27) was selected for analysis of DNA damage checkpoint function and global changes in gene expression. Although the three AT cell lines expressed little or no ATM protein and displayed attenuated DNA damage checkpoint functions, they nevertheless displayed redistribution among the cell cycle compartments after IR treatment. The patterns of redistribution were consistent with IR-induced cell cycle delays in G1 and G2. The G1 delay produced a reduction in S phase cells; the G2 delay produced a reduction in mitotic cells. The dynamic changes in the G1, S and G2 compartments from 2–24 h after irradiation were similar in the three cell lines. Mitosis was also repressed from 2–24 h in two of the lines with a third displaying recovery of mitosis at 24 h. This finding demonstrated that there were idiosyncratic differences in responses to DNA damage among the three AT cell lines. The results of analysis of global gene expression in IR-treated AT cells also revealed non-stereotypic responses patterns among the AT cell lines.

Two methods were used to analyze microarray data in AT cell lines. In one, expression profiles from the three AT lines were analyzed to identify stereotypic responses shared by all of the lines. EPIG analysis extracted 4 expression patterns and 349 genes. It was noted from this analysis that many p53 target genes, such as *CDKN1A, GADD45A2, BTG2, BAX* and *DDB2*, and many G2/M transition-regulated genes, such as *CCNB1, CCNB2, CDC20, CDC25C* and *TOP2A*, were not identified. In previous studies of this type (22, 30) these genes displayed attenuated or delayed responses to IR in AT cells. In order to identify as many IR-responsive genes as possible in AT patients, sets of two of the three AT lines were used for extraction of expression patterns and identification of significant genes. In this way the p53 target genes were recognized in the AT2 and AT3 combination, and the G2/M transition-regulated genes were identified in AT1 and AT3 combination. This analysis showed that AT1 was deficient in late induction of p53 target genes, which may lead to the lack of late repression of some cell cycle-regulated genes, such as *CDC6, CDCA7, FANCE, MSH6* and *UNG* in this cell line (Figure 5, pattern 3), and AT2 was deficient in late repression of G2/M transition-regulated genes, which was associated with the marked recovery from G2 arrest at 24 h post-IR in AT2 cells. These results explained why the p53 target genes and G2/M transition-regulated genes were not identified when expression data from all three cell lines were used for EPIG analysis.

When compared with gene expression profiles in normal fibroblasts, 715 genes were also commonly changed by IR in AT fibroblasts, including many genes that are related to cell cycle regulation and DNA damage response. However, the changes of these genes differed between normal and AT cell lines in patterns and degree of change. For example, while *CDKN1A, FDXR, SNK, PLAB* and *DDB2* all were rapidly induced after IR in normal fibroblasts (27), these genes displayed delayed induction in AT cell lines. Analysis of global gene expression confirmed previous results that DNA damage responses do occur in AT cells given a large enough dose or enough time post-treatment (28). Another study of global gene expression in AT cells demonstrated rapid induction of p53 target genes after high doses of IR (30). ATM and ATR can phosphorylate the same target genes (38), and inactivation of ATR function has been shown to attenuate DNA damage checkpoint response to IR (39, 40). Further, it is suggested that when RPA coats single-stranded DNA intermediates that are produced during repair of DNA DSB, ATR is activated to phosphorylate checkpoint effector genes such as p53 and Chk1(41). Therefore it is reasonable to conclude that ATR signals from sites of IR-induced DNA damage to induce

DNA damage checkpoint responses and global changes in gene expression in normal and AT cells (Figure 6).

There were 1096 genes that responded to DNA damage in normal cells but not in AT cells. Many of these genes display delayed repression associated with prolonged G1 arrest or delayed induction associated with development of a G0-like state of quiescence (27). Because the irradiated AT cells did not fully arrest cell division in G1 or G2, but rather continued to move through G1 and G2, albeit at reduced rates, they did not enter the G0-like state of quiescence as normal cells did, and many cycle-regulated genes probably did not achieve the signal-to-noise ratio threshold needed to be identified as significant genes.

EPIG also identified 306 genes that responded to IR in AT cells but not in normal cells and gene ontology analysis yielded two over-represented biological categories, cell communication and morphogenesis. Although AT cells display reduced DNA damage checkpoint function in comparison to normal, they display enhanced cytotoxicity as was reproduced with the telomerase-expressing AT lines. After the 1.5 Gy dose of IR used in these studies, 90% of AT fibroblasts were killed or permanently arrested, but only 40% of normal fibroblasts experienced such effects. It is plausible that AT cells recognize the greater level of lethal cellular damage and trigger responses not seen in the normal cells. The data suggest that AT fibroblasts might respond to lethal damage with changes in cell communication and morphogenesis.

Analysis of the dynamic changes in cell cycle compartments showed a nearly 3-fold increase in the proportion of G2 phase AT cells at 24 h after IR-treatment. Genes that regulate the G2/M transition and are induced in late S and G2 such as *CDC2, CCNB1, CCNB2*, and *CDC20* were repressed in irradiated AT1 and AT3 cell lines. p53 has been shown to repress the expression of *CDC2, CCNB1* and *CCNB2* (42, 43), and analysis of global gene expression in normal fibroblasts suggested that many cell-cycle-regulated genes were repressed in response to IR-induced DNA damage through a p53-dependent pathway (27). The repression of these genes in irradiated AT cells suggests the contribution of an ATM-independent but p53-dependent pathway to induce G2 delay. This pathway was not recognized in the AT2 cell line, suggesting that the AT2 line has an idiosyncratic alteration affecting its response to DNA damage (Figure 6). Interestingly, although the late repression of *CDC2, CCNB1, CCNB2*, and *CDC20* was observed in the AT1 cell line, it displayed a defect in the induction of p53 targets, such as *CDKN1A, GADD45A, BTG2* and *DDB2* (Figure 6). This suggests there also may be a p53-independent pathway to repress G2/M transition genes. The lack of induction of the canonical p53 targets may also be related to the ablated late repression of genes associated with regulation of the G1/S transition and DNA repair, such as *CDC6, MSH6* and *UNG* in AT1 cells (Figure 5, pattern 3).

Consistent with the severely reduced expression of ATM, significant defects in DNA damage checkpoint response and markedly increased radiosensitivity in the three AT cell lines, changes in global gene expression profiles of AT cells, when compared with normal cells, revealed ATM-dependent and ATM-independent stereotypic gene regulation in response to IR-induced DNA damage. Upon IR-induced DNA damage, induction of early DNA damage-responsive genes, especially *CDKN1A*, is critical to establish G1 arrest (1) and active trans-repression of cell cycle regulated genes, especially those functioning in G2/M transition, is also important for maintenance of the G2 arrest (Zhou et al., in press). Lack of immediate ATM- and p53-dependent induction of *CDKN1A* and decreased active repression of G2/M transition-regulated genes at least partially contributed to the observed attenuations of the G1 and G2 checkpoints, allowing cells with damaged DNA proceed through the cell cycle. The G1/S checkpoint seems to be critical for avoiding mutation after DNA damage but does not have significant effect on cell survival (44). However, failure in

activation and maintenance of the G2/M checkpoint would allow IR-damaged G2 phase cells to proceed into mitosis carrying unrepaired DNA double strand breaks causing a subsequent permanent arrest in G1 through the p53-dependent pathway (44). The observation that p53-deficient fibroblasts with ablated G1 checkpoint function but effective G2 checkpoint function are radio-resistant supports this hypothesis(45). Defective regulation of the G2 checkpoint in AT cells, at both transcriptional and post-transcriptional levels, may contribute to the phenotype of radiosensitivity.

Moreover, idiosyncratic responses of global gene expression profiles upon DNA damage in individual AT cell lines suggest that some ATM mutations may cause defects in DNA damage response by mechanisms in addition to the common well-reported defects in checkpoint functions. There are over 400 disease-associated mutations in ATM and no hot spots for mutation (8). The idiosyncratic changes in global gene expression may reflect the underlying genetic instability associated with ATM deficiency that leads to different phenotypes in AT patients (31), and may help us subclassify AT patients for better treatment.

Materials and methods

Cell lines and culture

AT fibroblast strains, GM02052A (AT1), GM08391 (AT2) and GM03395 (AT3) were obtained from the Coriell Institute (Camden, NJ). Normal human fibroblast strains, F1, F3 and F10, were derived from neonatal foreskins and established in secondary culture according to established methods (46). Immortalized cell lines were obtained by ectopic expression of human telomerase (hTERT), as previously described (40, 47). AT1 and AT2 were cultured in DMEM high glucose medium supplemented with 2 mM L-glutamine and 20% fetal bovine serum (FBS) and displayed typical fibroblastic growth in culture with spreading of spindle-shaped cells to cover the dishes. However, the AT3 line was anomalous and grew in clumps without spreading on culture dishes in the standard AT fibroblast growth medium. Therefore, AT3 was cultured in AmnioMAX™-C100 medium (450 ml basal medium +15 ml supplement) (Invitrogen, Carlsbad, CA) with 10% FBS. In this medium AT3 assumed the typical spindle morphology of fibroblasts with spreading growth to cover culture dishes. All experiments with AT3 were done with Amniomax supplementation of growth medium. The normal human fibroblast lines were cultured in DMEM high glucose medium supplemented with 2 mM L-glutamine and 10% or 20% fetal bovine serum. All cell lines were maintained at 37°C in a humidified atmosphere of 5% CO_2 and were routinely tested and shown to be free of mycoplasma contamination using a commercial assay (Gen-Probe, San Diego, CA).

Western blotting

Logarithmically growing AT and normal fibroblasts were harvested by trypsinization, washed once in phosphate-buffered saline, and resuspended in lysis buffer (10 mM sodium phosphate buffer [pH 7.2], 1 mM EDTA, 1 mM EGTA, 150 mM NaCl, and 1% NP-40, supplemented with 10 mM 4-(2-aminoethyl) benzenesulfonyl fluoride, 10 mM β-glycerophosphate, 10 mM sodium orthovanadate, and 10 μg/ml concentrations of leupeptin and aprotinin). Protein concentrations were determined using the Bio-Rad D_C protein assay (Bio-Rad Laboratories). Samples containing equal amounts (100 μg) of protein were mixed with an equal volume of 2x Laemmli sample buffer (125 mM Tris-HCl [pH 6.8], 4% sodium dodecyl sulfate [SDS], 20% glycerol) containing 5% β-mercaptoethanol, boiled, and separated by SDS-polyacrylamide gel electrophoresis (SDS-PAGE). Proteins were transferred to nitrocellulose and probed with antibodies against ATM. Production of affinity-purified anti-ATM antibody was previously described (48).

Cell irradiation

Cells were exposed to ionizing radiation in their culture medium, using a ^{137}Cs source (Gammacell 40, Atomic Energy of Canada Ltd., Ottawa, Canada) at a dose rate of 0.84 Gy/min. Sham-treated controls were subjected to the same movements in and out of incubators as irradiated cells.

Clonogenic assay

Colony formation was measured in logarithmically growing AT1, AT2 and AT3 fibroblasts, plated at 1000–1200 cells per 100 mm diameter dish and incubated for 8 hours before exposure to IR (3 dishes per dose). Cells were cultured for 2 weeks, changing medium twice a week. Colonies were fixed and stained with a solution of 40% methanol and 0.05% crystal violet. Colonies with ≥50 cells were counted. The relative colony forming efficiency of IR-treated cells was expressed as a fraction of sham-treated controls.

Cell cycle checkpoint assays

Logarithmically growing AT cells were seeded at $5x10^5$ per 100-mm dish, fed at 24 h and irradiated 48 h after seeding as described above. For quantitative analysis of the G1 checkpoint, 10 μM 5'-bromo-2'-deoxyuridine (BrdU, Sigma Chemical Co., St. Louis, MO) was added to culture medium at various times after irradiation to label S phase cell DNA and cultures were incubated for another 2 hours. Cells were harvested, washed with phosphate-buffered saline (PBS), and fixed with 67% ethanol in PBS. Cells were stained with fluorescein isothiocyanate (FITC)-conjugated anti-BrdU antibody (BD Biosciences, San Jose, CA) and propidium iodide (PI, Sigma) then S phase cells were enumerated by flow cytometry as previously described (10, 49, 50). For quantitative analysis of the G2 checkpoint, mitotic cells were quantified by flow cytometry. Briefly, cells were harvested at various times after irradiation, washed with PBS, fixed in 1% formaldehyde in PBS for 30 min, and then fixed in 67% ethanol in PBS. Cells were incubated in 0.5 μg/100μl anti-phospho-histone H3 antibody (Upstate Biotechnology, Lake Placid, NJ) for 2 h, and then stained with FITC-conjugated anti-rabbit antibody (Santa Cruz Biotechnology, Santa Cruz, CA) and propidium iodide (51–53). Flow cytometric analyses to enumerate mitotic cells were done using a FACScan flow cytometer (BD, San Jose, CA) and Summit software (Dako Colorado Inc., Fort Collins, CO).

Oligo DNA Microarray

Logarithmically growing AT cells were treated with 1.5 Gy IR and harvested at 2, 6 or 24 h after the treatment. Controls were harvested 6 h after sham treatment. Total RNA was isolated using Qiagen RNeasy kit (Qiagen Sciences, Germantown, MD). The quality of all RNA samples was confirmed using an Agilent 2100 Bioanalyzer (Agilent Technologies, Palo Alto, CA). Microarray analysis was then performed using a 22,000 element human 1A array (Agilent) through a contract with Cogenics Inc. (Research Triangle Park, NC). For details, please refer to our previous publication (27).

Microarray data analysis

The extraction of gene expression patterns and identification of significantly changed genes were carried out using a method known as EPIG (27). Three parameters, the correlation coefficient within a specific pattern, the magnitude of change in gene expression (signal), and the signal-to-noise ratio (SNR), were employed for selection of significant genes (27).

Two strategies were used for extraction of IR-responding genes in AT cells. First, all three AT cell lines were analyzed to see the stereotypic gene changes in AT cells. Second, two of three AT cell lines with combinations of AT1/AT2, AT2/AT3, and AT1/AT3 were analyzed

to see the diversity in gene changes among AT cells that may have different mutations and respond to IR differently. Results from the second analysis were compared with IR-responding genes in normal human fibroblasts (30).

Gene ontology categories that were over-represented in a selected gene list, compared to what was represented on the microarray, were identified using **E**xpression **A**nalysis **S**ystematic **E**xplorer (EASE). Such over-represented categories represent biological "themes" of a given list (http://apps1.niaid.nih.gov/david/).

Acknowledgments

We thank Jennifer Helms for performing tests for mycoplasma contamination, George Wu for helping with microarray data analysis and database management. We acknowledge PHS's contribution of the Software EASE used in our data analysis.

Supported in part by PHS grants ES10126 and ES11391.

References

1. Abraham RT. Cell cycle checkpoint signaling through the ATM and ATR kinases. Genes Dev. 2001; 15(17):2177–2196. [PubMed: 11544175]
2. Shiloh Y. ATM and ATR: networking cellular responses to DNA damage. Curr Opin Genet Dev. 2001; 11(1):71–77. [PubMed: 11163154]
3. Baross A, Schertzer M, Zuyderduyn SD, Jones SJ, Marra MA, Lansdorp PM. Effect of TERT and ATM on gene expression profiles in human fibroblasts. Genes Chromosomes Cancer. 2004; 39(4): 298–310. [PubMed: 14978791]
4. Bakkenist CJ, Kastan MB. DNA damage activates ATM through intermolecular autophosphorylation and dimer dissociation. Nature. 2003; 421(6922):499–506. [PubMed: 12556884]
5. Concannon P, Gatti RA. Diversity of ATM gene mutations detected in patients with ataxia-telangiectasia. Hum Mutat. 1997; 10(2):100–107. [PubMed: 9259193]
6. Fernet M, Moullan N, Lauge A, Stoppa-Lyonnet D, Hall J. Cellular responses to ionising radiation of AT heterozygotes: differences between missense and truncating mutation carriers. Br J Cancer. 2004; 90(4):866–873. [PubMed: 14970866]
7. Thorstenson YR, Shen P, Tusher VG, et al. Global analysis of ATM polymorphism reveals significant functional constraint. Am J Hum Genet. 2001; 69(2):396–412. [PubMed: 11443540]
8. Campbell C, Mitui M, Eng L, Coutinho G, Thorstenson Y, Gatti RA. ATM mutations on distinct SNP and STR haplotypes in ataxia-telangiectasia patients of differing ethnicities reveal ancestral founder effects. Human mutation. 2003; 21(1):80–85. [PubMed: 12497634]
9. Falck J, Mailand N, Syljuasen RG, Bartek J, Lukas J. The ATM-Chk2-Cdc25A checkpoint pathway guards against radioresistant DNA synthesis. Nature. 2001; 410(6830):842–847. [PubMed: 11298456]
10. Kaufmann WK, Heffernan TP, Beaulieu LM, et al. Caffeine and human DNA metabolism: the magic and the mystery. Mutat Res. 2003; 532(1–2):85–102. [PubMed: 14643431]
11. Lavin MF, Shiloh Y. The genetic defect in ataxia-telangiectasia. Annu Rev Immunol. 1997; 15:177–202. [PubMed: 9143686]
12. Pandita TK. The role of ATM in telomere structure and function. Radiat Res. 2001; 156(5 Pt 2): 642–647. [PubMed: 11604086]
13. Chen S, Wang G, Makrigiorgos GM, Price BD. Stable siRNA-mediated silencing of ATM alters the transcriptional profile of HeLa cells. Biochem Biophys Res Commun. 2004; 317(4):1037–1044. [PubMed: 15094373]
14. Shi Y, Venkataraman SL, Dodson GE, Mabb AM, LeBlanc S, Tibbetts RS. Direct regulation of CREB transcriptional activity by ATM in response to genotoxic stress. Proc Natl Acad Sci U S A. 2004; 101(16):5898–5903. [PubMed: 15073328]

15. Niedernhofer LJ, Garinis GA, Raams A, et al. A new progeroid syndrome reveals that genotoxic stress suppresses the somatotroph axis. Nature. 2006; 444(7122):1038–1043. [PubMed: 17183314]
16. Hasty P, Campisi J, Hoeijmakers J, van Steeg H, Vijg J. Aging and genome maintenance: lessons from the mouse? Science. 2003; 299(5611):1355–1359. [PubMed: 12610296]
17. Herbig U, Jobling WA, Chen BP, Chen DJ, Sedivy JM. Telomere shortening triggers senescence of human cells through a pathway involving ATM, p53, and p21(CIP1), but not p16(INK4a). Mol Cell. 2004; 14(4):501–513. [PubMed: 15149599]
18. Vaziri H, West MD, Allsopp RC, et al. ATM-dependent telomere loss in aging human diploid fibroblasts and DNA damage lead to the post-translational activation of p53 protein involving poly(ADP-ribose) polymerase. Embo J. 1997; 16(19):6018–6033. [PubMed: 9312059]
19. Naka K, Tachibana A, Ikeda K, Motoyama N. Stress-induced premature senescence in hTERT-expressing ataxia telangiectasia fibroblasts. J Biol Chem. 2004; 279(3):2030–2037. [PubMed: 14570874]
20. Verdun RE, Crabbe L, Haggblom C, Karlseder J. Functional human telomeres are recognized as DNA damage in G2 of the cell cycle. Mol Cell. 2005; 20(4):551–561. [PubMed: 16307919]
21. Elkon R, Rashi-Elkeles S, Lerenthal Y, et al. Dissection of a DNA-damage-induced transcriptional network using a combination of microarrays, RNA interference and computational promoter analysis. Genome Biol. 2005; 6(5):R43. [PubMed: 15892871]
22. Heinloth AN, Shackelford RE, Innes CL, et al. ATM-dependent and -independent gene expression changes in response to oxidative stress, gamma irradiation, and UV irradiation. Radiat Res. 2003; 160(3):273–290. [PubMed: 12926986]
23. Stankovic T, Hubank M, Cronin D, et al. Microarray analysis reveals that TP53- and ATM-mutant B-CLLs share a defect in activating proapoptotic responses after DNA damage but are distinguished by major differences in activating prosurvival responses. Blood. 2004; 103(1):291–300. [PubMed: 12958068]
24. Watts JA, Morley M, Burdick JT, et al. Gene expression phenotype in heterozygous carriers of ataxia telangiectasia. Am J Hum Genet. 2002; 71(4):791–800. [PubMed: 12226795]
25. Taylor AM, Harnden DG, Arlett CF, et al. Ataxia telangiectasia: a human mutation with abnormal radiation sensitivity. Nature. 1975; 258(5534):427–429. [PubMed: 1196376]
26. Arlett CF, Green MH, Priestley A, Harcourt SA, Mayne LV. Comparative human cellular radiosensitivity: I. The effect of SV40 transformation and immortalisation on the gamma-irradiation survival of skin derived fibroblasts from normal individuals and from ataxia-telangiectasia patients and heterozygotes. Int J Radiat Biol. 1988; 54(6):911–928. [PubMed: 2903889]
27. Zhou T, Chou JW, Simpson DA, et al. Profiles of global gene expression in ionizing-radiation-damaged human diploid fibroblasts reveal synchronization behind the G1 checkpoint in a G0-like state of quiescence. Environ Health Perspect. 2006; 114(4):553–559. [PubMed: 16581545]
28. Canman CE, Wolff AC, Chen CY, Fornace AJ Jr, Kastan MB. The p53-dependent G1 cell cycle checkpoint pathway and ataxia-telangiectasia. Cancer Res. 1994; 54(19):5054–5058. [PubMed: 7923116]
29. Dulic V, Kaufmann WK, Wilson SJ, et al. p53-dependent inhibition of cyclin-dependent kinase activities in human fibroblasts during radiation-induced G1 arrest. Cell. 1994; 76(6):1013–1023. [PubMed: 8137420]
30. Innes CL, Heinloth AN, Flores KG, et al. ATM requirement in gene expression responses to ionizing radiation in human lymphoblasts and fibroblasts. Mol Cancer Res. 2006; 4(3):197–207. [PubMed: 16547157]
31. Taylor AM, Byrd PJ. Molecular pathology of ataxia telangiectasia. Journal of clinical pathology. 2005; 58(10):1009–1015. [PubMed: 16189143]
32. Peretz S, Jensen R, Baserga R, Glazer PM. ATM-dependent expression of the insulin-like growth factor-I receptor in a pathway regulating radiation response. Proc Natl Acad Sci U S A. 2001; 98(4):1676–1681. [PubMed: 11172010]
33. Yang DQ, Kastan MB. Participation of ATM in insulin signalling through phosphorylation of eIF-4E-binding protein 1. Nat Cell Biol. 2000; 2(12):893–898. [PubMed: 11146653]

34. Grimberg A, Cohen P. Role of insulin-like growth factors and their binding proteins in growth control and carcinogenesis. Journal of cellular physiology. 2000; 183(1):1–9. [PubMed: 10699960]
35. Busiguina S, Fernandez AM, Barrios V, et al. Neurodegeneration is associated to changes in serum insulin-like growth factors. Neurobiol Dis. 2000; 7(6 Pt B):657–665. [PubMed: 11114263]
36. Fang NY, Greiner TC, Weisenburger DD, et al. Oligonucleotide microarrays demonstrate the highest frequency of ATM mutations in the mantle cell subtype of lymphoma. Proc Natl Acad Sci U S A. 2003; 100(9):5372–5377. [PubMed: 12697903]
37. Jang ER, Lee JH, Lim DS, Lee JS. Analysis of ataxia-telangiectasia mutated (ATM)- and Nijmegen breakage syndrome (NBS)-regulated gene expression patterns. J Cancer Res Clin Oncol. 2004; 130(4):225–234. [PubMed: 14745549]
38. Kim ST, Lim DS, Canman CE, Kastan MB. Substrate specificities and identification of putative substrates of ATM kinase family members. J Biol Chem. 1999; 274(53):37538–37543. [PubMed: 10608806]
39. Cliby WA, Roberts CJ, Cimprich KA, et al. Overexpression of a kinase-inactive ATR protein causes sensitivity to DNA-damaging agents and defects in cell cycle checkpoints. Embo J. 1998; 17(1):159–169. [PubMed: 9427750]
40. Deming PB, Cistulli CA, Zhao H, et al. The human decatenation checkpoint. Proc Natl Acad Sci U S A. 2001; 98(21):12044–12049. [PubMed: 11593014]
41. Bekker-Jensen S, Lukas C, Kitagawa R, et al. Spatial organization of the mammalian genome surveillance machinery in response to DNA strand breaks. The Journal of cell biology. 2006; 173(2):195–206. [PubMed: 16618811]
42. Taylor WR, Stark GR. Regulation of the G2/M transition by p53. Oncogene. 2001; 20(15):1803–1815. [PubMed: 11313928]
43. Taylor WR, DePrimo SE, Agarwal A, et al. Mechanisms of G2 arrest in response to overexpression of p53. Mol Biol Cell. 1999; 10(11):3607–3622. [PubMed: 10564259]
44. Marples B, Wouters BG, Collis SJ, Chalmers AJ, Joiner MC. Low-dose hyper-radiosensitivity: a consequence of ineffective cell cycle arrest of radiation-damaged G2-phase cells. Radiat Res. 2004; 161(3):247–255. [PubMed: 14982490]
45. Cistulli CA, Kaufmann WK. p53-dependent signaling sustains DNA replication and enhances clonogenic survival in 254 nm ultraviolet-irradiated human fibroblasts. Cancer Res. 1998; 58(9):1993–2002. [PubMed: 9581844]
46. Maher VM, Heflich RH, McCormick JJ. Repair of DNA damage induced in human fibroblasts by N-substituted aryl compounds. Natl Cancer Inst Monogr. 1981; (58):217–222. [PubMed: 7341979]
47. Heffernan TP, Simpson DA, Frank AR, et al. An ATR- and Chk1-dependent S checkpoint inhibits replicon initiation following UVC-induced DNA damage. Mol Cell Biol. 2002; 22(24):8552–8561. [PubMed: 12446774]
48. Shackelford RE, Innes CL, Sieber SO, Heinloth AN, Leadon SA, Paules RS. The Ataxia telangiectasia gene product is required for oxidative stress-induced G1 and G2 checkpoint function in human fibroblasts. J Biol Chem. 2001; 276(24):21951–21959. [PubMed: 11290740]
49. Kastan MB, Onyekwere O, Sidransky D, Vogelstein B, Craig RW. Participation of p53 protein in the cellular response to DNA damage. Cancer Res. 1991; 51(23 Pt 1):6304–6311. [PubMed: 1933891]
50. Kaufmann WK, Schwartz JL, Hurt JC, et al. Inactivation of G2 checkpoint function and chromosomal destabilization are linked in human fibroblasts expressing human papillomavirus type 16 E6. Cell Growth Differ. 1997; 8(10):1105–1114. [PubMed: 9342189]
51. Juan G, Traganos F, James WM, et al. Histone H3 phosphorylation and expression of cyclins A and B1 measured in individual cells during their progression through G2 and mitosis. Cytometry. 1998; 32(2):71–77. [PubMed: 9627219]
52. Kaufmann WK, Levedakou EN, Grady HL, Paules RS, Stein GH. Attenuation of G2 checkpoint function precedes human cell immortalization. Cancer Res. 1995; 55(1):7–11. [PubMed: 7805043]
53. Xu B, Kim ST, Lim DS, Kastan MB. Two molecularly distinct G(2)/M checkpoints are induced by ionizing irradiation. Mol Cell Biol. 2002; 22(4):1049–1059. [PubMed: 11809797]

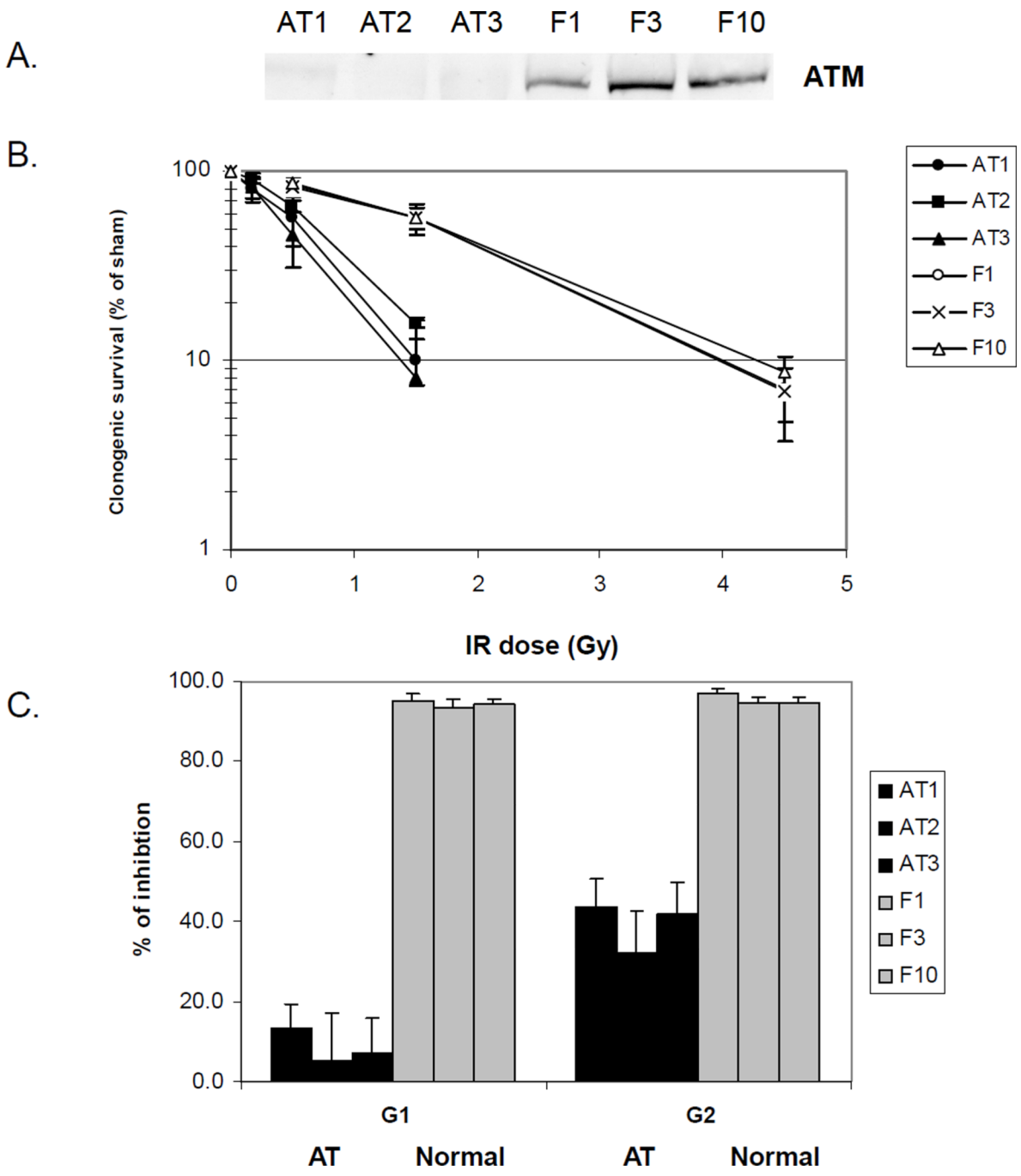

Figure 1.

A. Protein extracts were prepared from AT fibroblast cell lines (AT1, AT2 and AT3), and normal human fibroblast cell lines (F1, F3 and F10), and 100 μg of total protein was analyzed by western immunoblot analysis with anti-ATM antibody. B. Inactivation of clonogenic survival by IR. Three normal fibroblast lines and three AT fibroblast lines were irradiated with IR and colonies were counted after a 14-day incubation. Results show the mean relative colony formation in irradiated cultures (mean ± SD, n=3). C. IR-induced G1 and G2 checkpoint functions in normal and AT fibroblasts. Checkpoint functions were determined by measuring BrdU incorporation 6–8 h after 1.5 Gy IR or sham treatment (G1) and phospho-histone H3 expression 2 h after 1.5 Gy IR or sham treatments (G2) in normal

and AT cells. The values depicted for each fibroblast line are the mean percentages of inhibition of IR-treated cells relative to sham-treated cells (mean ± SD, n=3).

A

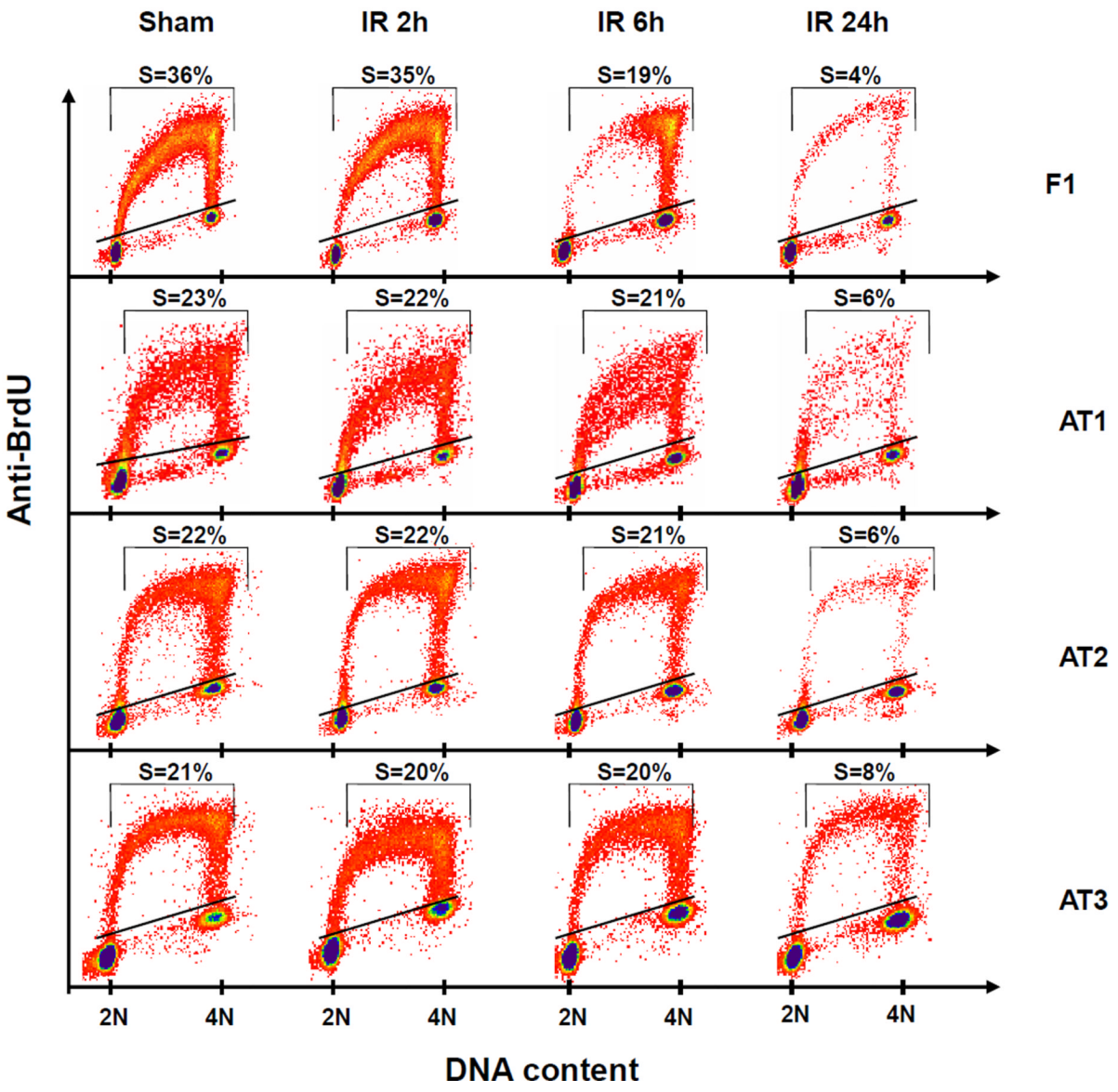

B

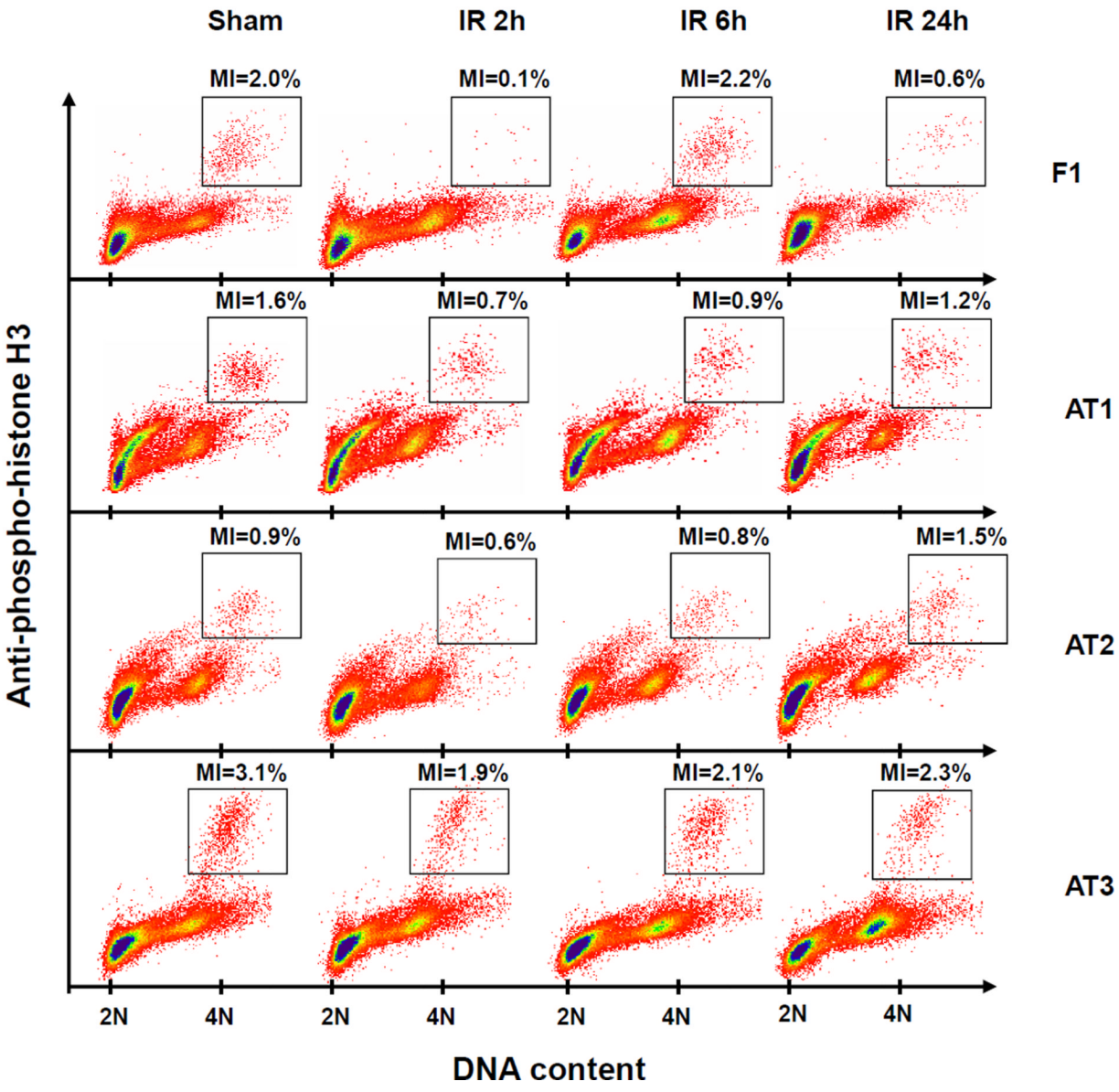

Figure 2.

The time-course of cellular DNA synthesis and mitosis in normal and AT cells after IR-induced DNA damage. A. The fractions of cells in S were determined by measuring BrdU incorporation with flow cytometry as described in Materials and Methods. B. Mitotic cells were quantified using anti-phospho-histone H3 antibody with flow cytometry. Although representative flow profiles are shown, the numerical values depicted for each cell line are the mean percentages of sham- or IR-treated cells in each cycle phase compartment (n=3). MI = mitotic index.

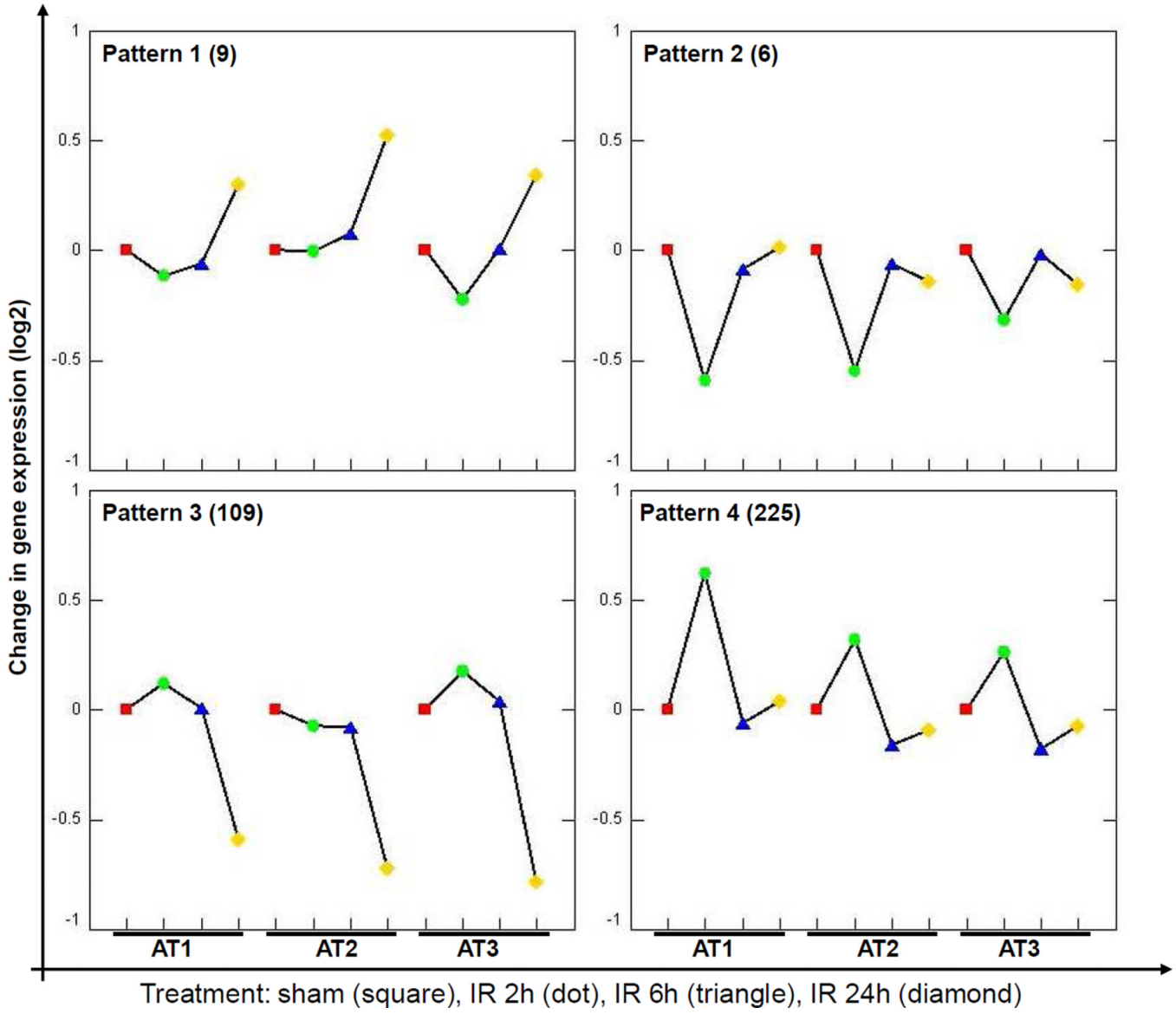

Figure 3.

Stereotypic gene expression patterns in AT cell lines in response to IR-induced DNA damage. Four DNA-damage-responsive patterns of gene expression were extracted using EPIG, each pattern represented a group of genes that responded to IR in the same way. Each pattern is presented as the average of the expression levels of the 6 most highly correlated genes, with the level of expression of each gene being the average of the two dye-flip replicates. For each pattern and for each cell line, gene expression levels are shown as the log2 ratios of sample RNA against reference RNA. The log2 ratio of gene expression in the sham-treated control was adjusted to zero and IR-treated samples were adjusted by the same proportion. Sample treatments from left to right were sham-treated control (square), IR 2h (circle), IR 6h (triangle) and IR 24h (diamond). In each panel, the numbers of genes in each pattern are shown in parentheses.

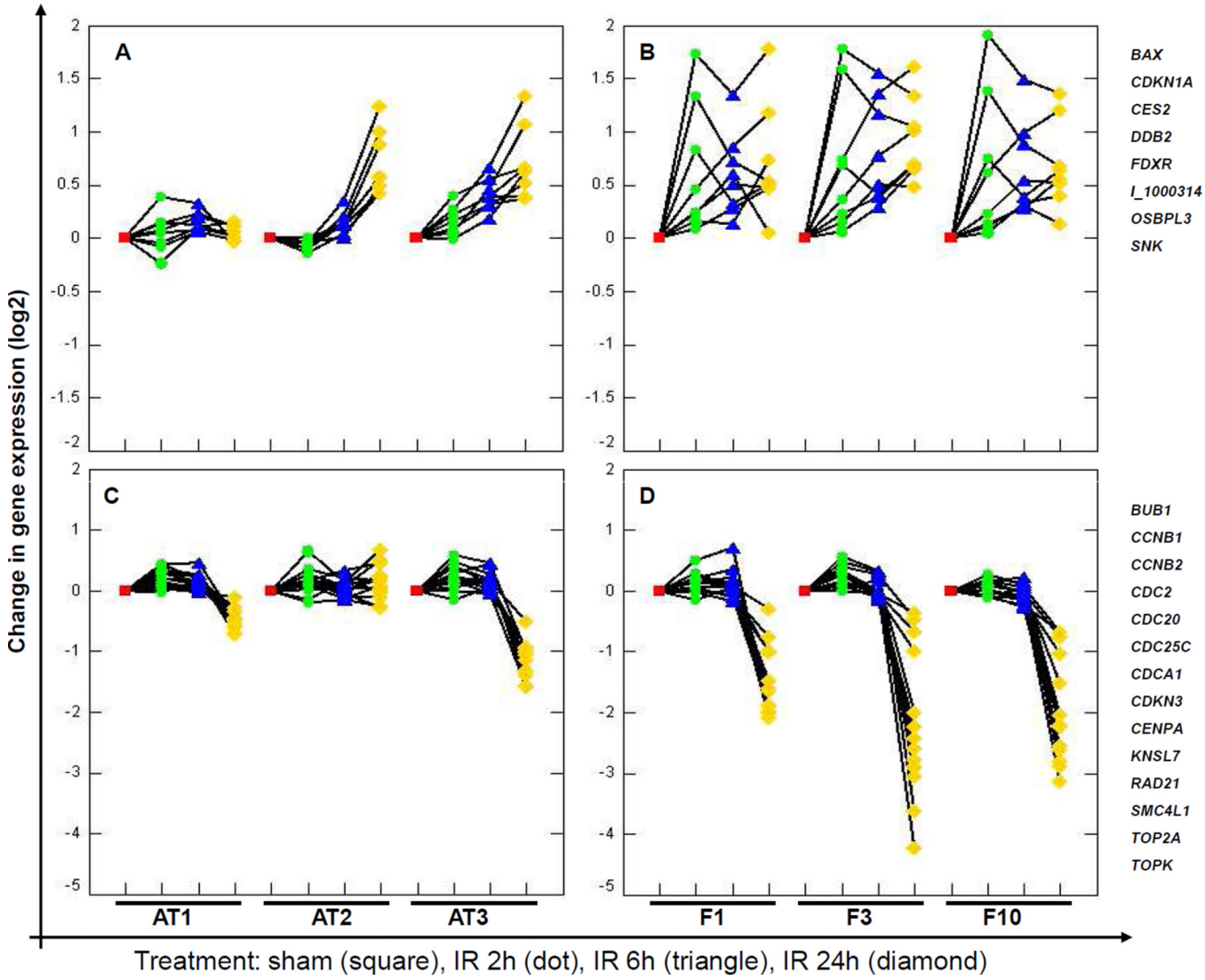

Figure 4.

Idiosyncratic expression of p53 targets or cell cycle-regulated genes in AT lines (AT1, AT2 and AT3) and stereotypic expression of these genes in normal lines (F1, F3 and F10). Details for each panel are as in Figure 3. Panels A and C show AT lines, panels B and D show normal lines. The names of the genes that were included in this analysis, including p53 target genes (A and B) and G2/M transition-regulated genes (C and D), are given on the right.

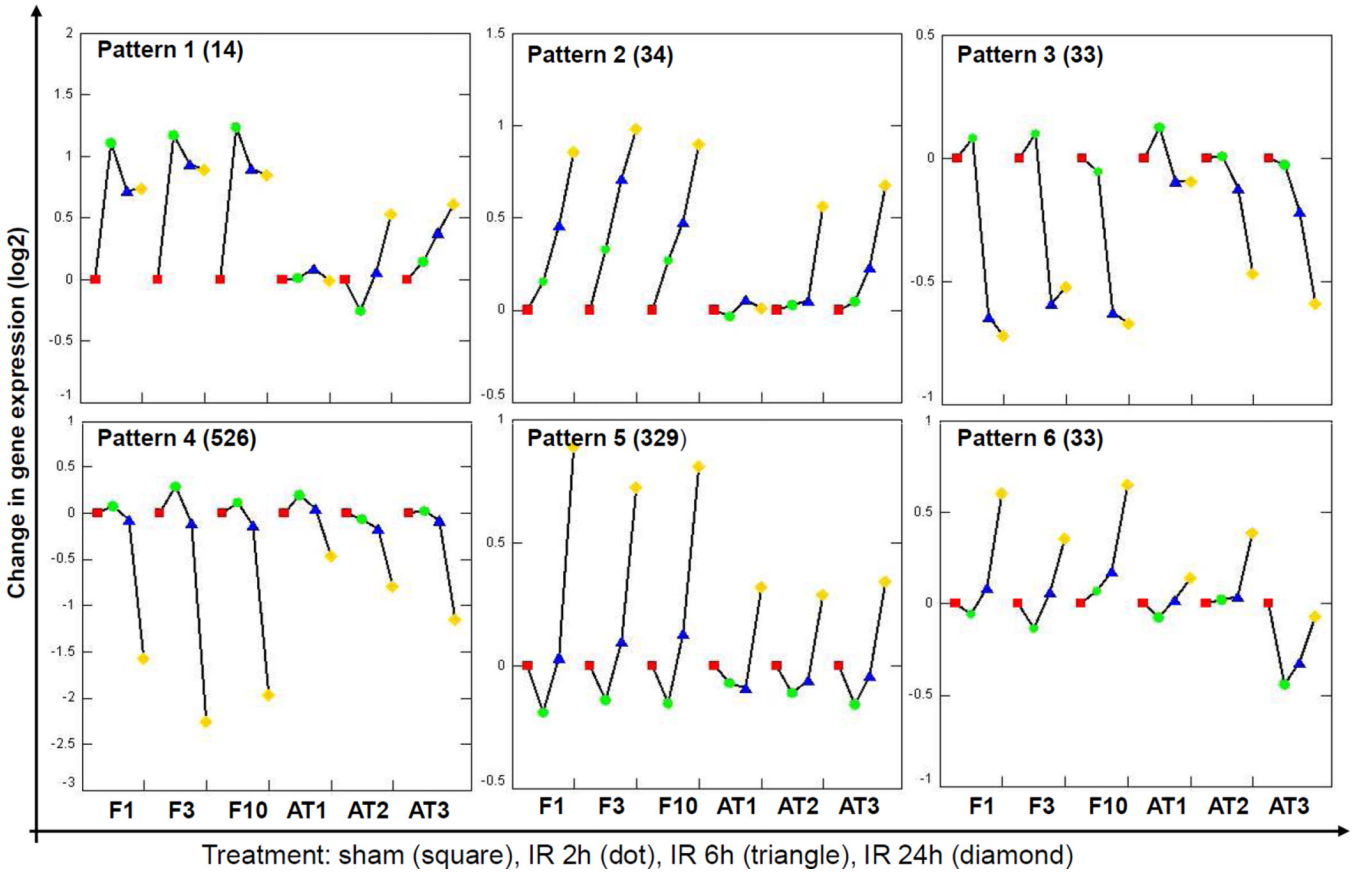

Figure 5.

ATM-dependent gene expression patterns in response to IR-induced DNA damage. Gene expression profiles for three AT cell lines and three normal cell lines were analyzed using EPIG. Six expression patterns were extracted showing different responses to IR between normal and AT cell lines. Each pattern is presented as the average of the expression levels of the 6 most highly correlated genes with the level of expression of each gene being the average of the two dye-flip replicates. In each panel, cell lines from left to right are F1, F3, F10, AT1, AT2 and AT3 as depicted at the bottom of the figure; the numbers of genes in each pattern are shown in parentheses. For each pattern and for each cell line, gene expression levels are as described in Figure 3.

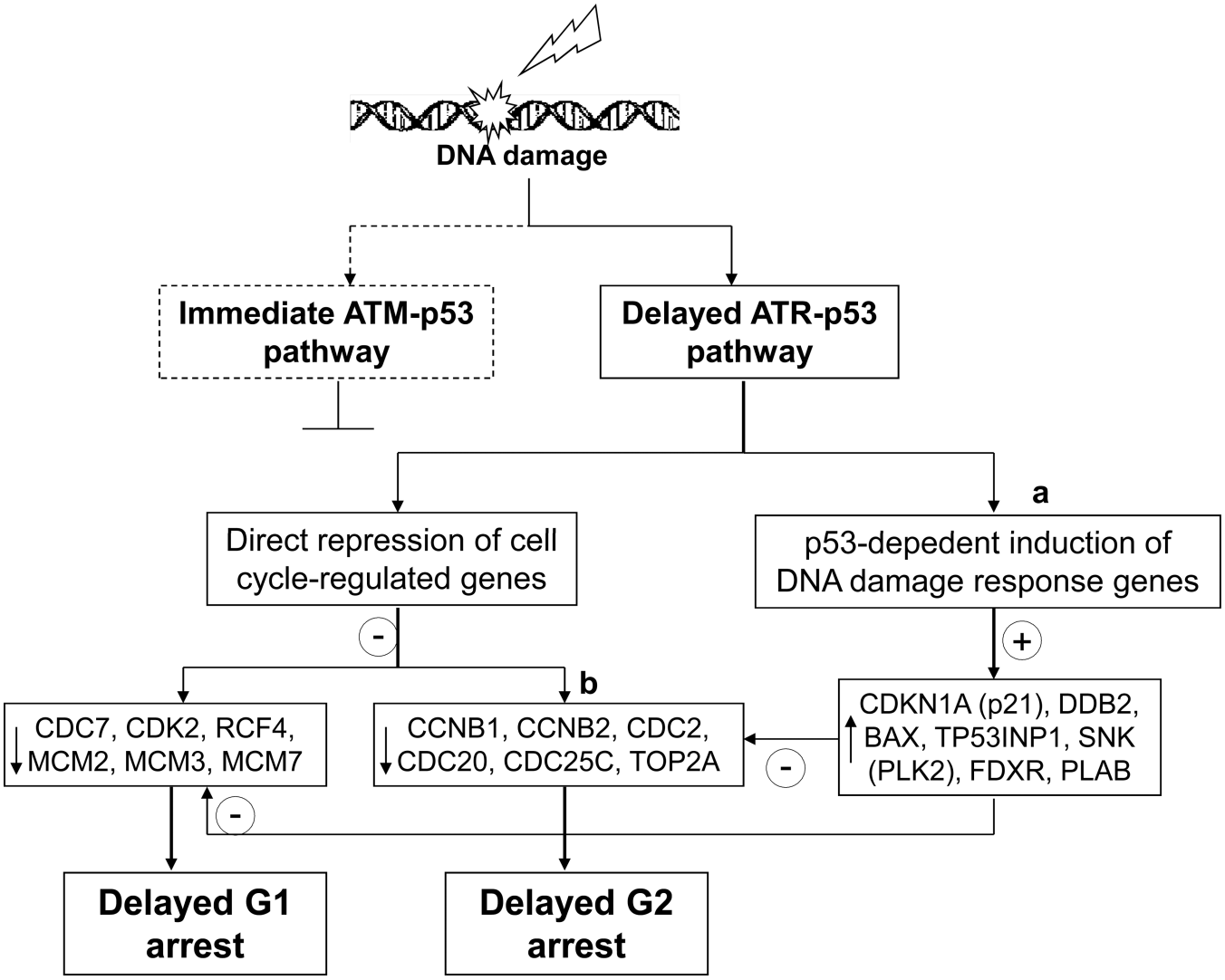

Figure 6.

Potential pathways of checkpoint function and cell cycle gene regulation in AT fibroblasts after IR-induced DNA damage. Upon IR-induced DNA damage, the ATM-dependent signaling pathway is absent in AT cells, but the ATR-dependent pathway, although delayed, is activated and initiates G1 and G2 arrests. p53 plays a key role in ATR-dependent cell cycle checkpoint function by inducing important cell cycle kinase inhibitors and by repressing transcription of cell cycle-regulated genes. Not all AT cell lines followed the same rules. The AT1 cell line was defective in induction of some p53 target genes, including $p21^{Waf1}$(a), and AT2 was defective in repression of G2/M transition-regulated genes upon DNA damage, leading to escape from delayed G2 arrest (b).